Robotic Compensation of Biological Motion to Enhance Surgical Accuracy

Cameron Riviere, *Member, IEEE*, Jacques Gangloff, *Member, IEEE*, and Michel de Mathelin, *Senior Member, IEEE*

***Abstract*—Robotic technologies provide new ways to compensate quasi-periodic biological motion, enabling higher surgical accuracy without invasive measures such as cardiopulmonary bypass. This paper describes current research in robotic compensation of hand tremor, respiratory motion, and heartbeat during surgical procedures. An analysis of each physiological motion pattern is provided, as well as a description of novel compensation techniques.**

***Index Terms*—Medical robotics, computer aided surgery, physiological motion compensation, tremor, respiration, heartbeat.**

I. Introduction

Involuntary quasi-periodic biological motion is a significant disturbance in the performance of a wide variety of medical and surgical procedures. Respiratory motion hinders accuracy throughout the thorax and abdomen, in laparoscopic procedures [1], cardiac interventions [2], percutaneous liver interventions [3], urologic surgery [4], radiotherapy [5, 6], and many other types of intervention.

The heartbeat is another major disturbance affecting surgical procedures. Its effect is somewhat more localized than that of respiration, but it still causes significant motion in much of the chest and parts of the upper abdomen, in addition to smaller cardioballistic effects elsewhere in the body as the blood is pumped through the arteries. The heart itself undergoes two different types of quasi-periodic motion, due to the respiration, and due to its own beating.

There are other types of localized involuntary quasi-periodic movement such as nystagmus, an uncontrolled movement of the eyes that must be accounted for (along with any other eye motion, involuntary or otherwise) during ophthalmological procedures such as laser *in situ* keratomileusis (LASIK) and laser photorefractive keratectomy [7, 8].

The effects listed above describe the involuntary movement of the patient. In addition to these, in tasks such as microsurgery, in which the requisite accuracy approaches the limits of human performance, the involuntary movement of the surgeon becomes a factor as well. Physiological tremor, a normal involuntary quasi-periodic movement that affects the hands of the surgeon, causes unsteadiness in instrument positioning during microsurgery, limiting the size of objects that can be manipulated [9, 10].

Current techniques to counteract quasi-periodic biological motion during surgery typically consist of either passive suppression or simply shutting down the disturbance source. For example, in cardiac surgery, the heart is often stopped, and cardiopulmonary bypass is used. Extracorporeal circulation has some major drawbacks, the most critical of which is a higher risk of neurological complications [11]. To avoid this problem, passive stabilizers have been developed, which use downward pressure or suction in an attempt to immobilize a small portion of the myocardium. Unfortunately, these can have significant residual motion, especially in a minimally invasive context [12].

In recent years robotic technologies have been investigated in order to provide more effective solutions to the problems of tremor, respiratory motion, and heartbeat during surgery. To this date, in general, most surgical robotic systems that have been developed operate in either a teleoperative or collaborative mode, keeping the surgeon in the loop. Active physiological motion compensation can be seen as a semi-autonomous mode, transparent to the surgeon, that uses an active mechanical device—i.e., a robot—to cancel unwanted motion while accurately following the command input given by the surgeon. Most of the projects described in this paper involve active compensation.

This paper presents current research in surgical accuracy enhancement through robotic compensation of hand tremor, respiratory motion, and heartbeat. An analysis of each type of motion is presented, followed by a description of novel compensation techniques developed in the authors' respective laboratories in Pittsburgh and Strasbourg. The effectiveness of the techniques is demonstrated *in vitro* and *in vivo*.

II. Physiological Tremor

Physiological hand tremor is classically said to have a dominant frequency of approximately 10 Hz, but in fact it contains various components whose frequency can range as high as 30 Hz [13]. This includes a "neurogenic" component of fixed frequency that appears to be generated within the central nervous system, and "mechanical-reflex" components

Manuscript received July 15, 2005, revised June 2, 2006. This work was supported in part by the U.S. National Institutes of Health under Grants R01 EB000526 and R01 HL078839, the National Science Foundation under Grant EEC-9731748, and the French national funding "ACI jeunes chercheurs."

C. Riviere is with the Robotics Institute, Carnegie Mellon University, Pittsburgh, PA 15213 USA (phone: 412-268-3083; fax: 412-268-7350; e-mail: camr@ri.cmu.edu).

J. Gangloff and M. de Mathelin are with the LSIIT laboratory, Strasbourg I University, France (phone: +33 3 90 24 44 68; fax: +33 3 90 24 44 80; e-mail: {jacques,demath}@eavr.u-strasbg.fr).

due to factors such as the dynamics of muscle fiber activation, cardioballistic effects, and the like, whose frequency depends on the mechanical properties of the body part in question [13]. Recent experiments in vitreoretinal surgical conditions have yielded an estimated frequency band of roughly 6-12 Hz, with typical amplitudes of 100 μm rms or less in each coordinate direction [14]. Physiological tremor is rather irregular in waveform (see Fig. 1) as opposed to, e.g., parkinsonian tremor which is much closer to a pure sinusoid. Gantert *et al.* [15] have presented results suggesting that it represents a linear stochastic process.

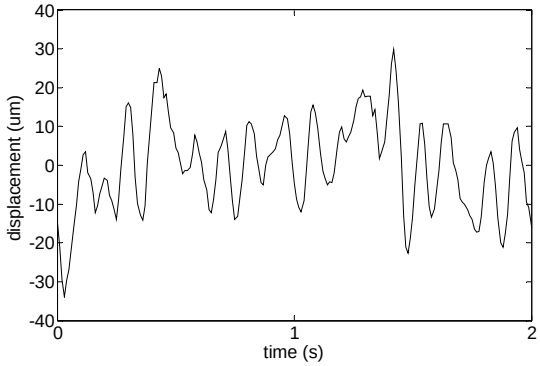

Fig. 1. Sample of physiological hand tremor recorded from the tip of a handheld microsurgical instrument.

The need to suppress hand tremor during microsurgery on, e.g., the retina, has been recognized for some time [10], and before surgery many surgeons take measures such as avoiding caffeine, ensuring plenty of sleep, and taking beta-blockers [16]. The amplitude of the remaining tremor is still significant for many microsurgical tasks, however, and technological solutions have been sought. Most attempts have involved teleoperation, the advantages of which include the facilitation of motion scaling and reflected force feedback, but these systems are complex and expensive [17-19]. The steady-hand robot [20] uses a shared-control approach, in which the surgeon's hand and the robot arm hold the same microsurgical tool, with the hand providing force input to the robot, which is programmed to resist those components of force that are understood to be tremor, and to comply with other components of force input.

Active compensation of tremor in a fully handheld microsurgical instrument is the goal of the Micron project in Dr. Riviere's laboratory [21]. A prototype of Micron is shown in Fig. 2. The instrument is designed to sense its own motion, distinguish tremor from other components of motion, and deflect its own tip to perform active compensation of the tremor.

Motion sensing is performed by a six-degree-of-freedom (6-dof) all-accelerometer inertial sensing module incorporated within the instrument [22]. Tip velocity is calculated and integrated to obtain a displacement signal.

Online estimation of tremor is performed using the weighted-frequency Fourier linear combiner (WFLC) algorithm developed by Riviere and Thakor [23] (a similar algorithm for the continuous-time case was developed

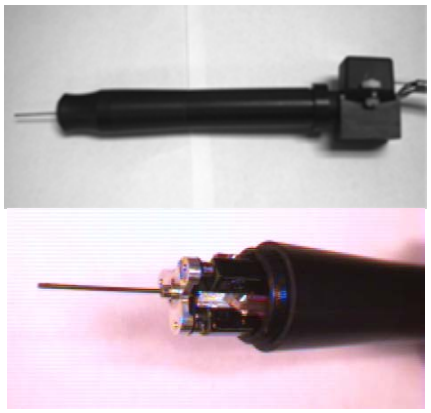

Fig. 2. Micron. The instrument senses its own motion using inertial sensing, performs adaptive filtering to estimate physiological tremor, and then deflects its tool tip (using the 3-dof manipulator shown in the lower photograph) to perform active compensation of the tremor.

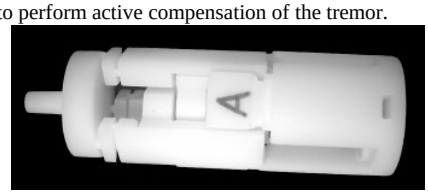

Fig. 3. New flexure-based manipulator recently developed for Micron, incorporating levers to provide fivefold mechanical amplification. The piezoelectric stacks fit into recessed chambers in the flexure; one chamber is visible at the lower right of the photograph.

independently by Bodson and Douglas [24, 25]). The algorithm forms a dynamic truncated Fourier series model of the tremor and adapts to track its changes in amplitude, frequency, and phase. In this case, because of the significant amount of non-tremulous movement also present, the WFLC is used with a bandpass prefilter to suppress the effects of the non-tremulous components, and the tremor frequency estimate from the WFLC is used to generate the reference oscillation for a second, separate FLC that operates without prefiltering to perform the online tremor estimation [26]. The equations of the overall WFLC-FLC system are [7]:

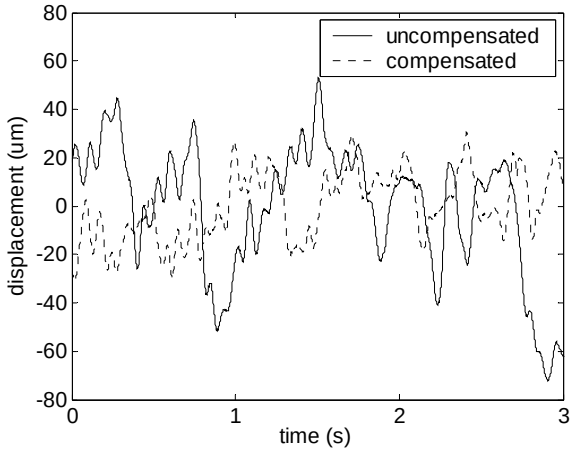

Fig. 4. Active tremor compensation *in vivo*, with Micron held in the hand of a human user. Tests with and without compensation are overlaid for comparison. The figure represents motion of the tool tip along a coordinate axis perpendicular to the long axis of the instrument.

$$x_{r_k} = \begin{cases} \sin\left[r \sum_{t=0}^{k} w_{0_t} \right], & 1 \le r \le M \\ \cos\left[(r-M) \sum_{t=0}^{k} w_{0_t} \right], & M+1 \le r \le 2M \end{cases} \quad (1)$$

$$\varepsilon_k = \tilde{s}_k - \mathbf{w}_k^T \mathbf{x}_k \quad (2)$$

$$w_{0_{k+1}} = w_{0_k} + 2\mu_0 \varepsilon_k \sum_{r=1}^{M} r\left(w_{r_k} x_{M+r_k} - w_{M+r_k} x_{r_k} \right) \quad (3)$$

$$\mathbf{w}_{k+1} = \mathbf{w}_k + 2\mu \mathbf{x}_k \varepsilon_k \quad (4)$$

$$\hat{\varepsilon}_k = s_k - \hat{\mathbf{w}}_k^T \mathbf{x}_k \quad (5)$$

$$\hat{\mathbf{w}}_{k+1} = \hat{\mathbf{w}}_k + 2\hat{\mu} \mathbf{x}_k \hat{\varepsilon}_k \quad (6)$$

where k is the time index, and $\mathbf{w}$ and $\hat{\mathbf{w}}$ are vectors of adaptive weights, each having length $2M$, s is the unfiltered input signal, and $\tilde{s}$ is the input signal after bandpass prefiltering with corner frequencies 7 and 14 Hz, as mentioned above. Equations (1)-(4) constitute the WFLC, and (5)-(6) are the second FLC used to avoid time delay. The tremor estimate, $\dot{y} = \hat{\mathbf{w}}_k^T \mathbf{x}_k$, is then used as a drive signal for the compensating actuators.

A 3-dof parallel manipulator is used to perform the active compensation of tremor (Fig. 2). The tremor estimate is used as input to the open-loop control system of the manipulator. Piezoelectric actuators are used because of their high bandwidth. The manipulator incorporates TS18-H5-202 piezoelectric stack actuators (Piezo Systems, Inc., Cambridge, Ma.), each of which measures 5 mm x 5 mm x 18 mm, with the long axis being the active dimension. These actuators offer good control linearity, maximum deflection of about 14 μm, response time of 50 μs, and actuation force of up to 840 N. In order to achieve the necessary range of motion, each axis of the manipulator is driven by a set of seven stacks placed in series.

Tests *in vitro* of the WFLC-based method using a simple 1-dof instrument yielded a 67% reduction in rms amplitude in the 6-16 Hz band [26]. In this case the input data were recordings of the movement of experienced eye surgeons as they attempted to hold an instrument motionless.

In tests *in vitro* of the full three-dimensional Micron prototype using a motorized testbed that generated an artificial quasi-sinusoidal disturbance, the instrument demonstrated average error reduction of 51% in twelve 1-dof (axial motion) trials, and 34% in twelve 3-dof trials [21].

In order to reduce size and weight while retaining a usable range of axial motion, we have recently designed a flexure-based tip manipulator incorporating lever assemblies for mechanical amplification (Fig. 3) [27]. Fig. 4 presents results from an experiment *in vivo* using the new manipulator. A small hole was made in a metal plate to simulate a sclerotomy port as is used for retinal surgery. A novice human subject inserted the tool shaft fully into the hole, and attempted to hold the tip motionless. Two trials were attempted, once with and once without compensation. The filter parameters used were M = 1, $\mathbf{w}_0$ = **0**, w_{0_0} = 0.6283 (10 Hz), Micron was controlled as in [21] (with μ=0.05, μ_0=10^{-6}, and $\hat{\mu}$ =0.1. The total range of the compensated motion was 52% less (60.8 μm compensated, 125.5 μm uncompensated) and the rms amplitude was 47% less (14.2 μm compensated, 26.7 μm uncompensated).

III. Respiratory Motion

Many medical interventions could be improved by respiratory motion compensation. In particular, minimally invasive procedures such as radiotherapy, percutaneous surgery, and laparoscopic surgery stand to benefit greatly, due to the difficulty of passively stabilizing organs without the easier access that open surgery provides.

A distinction must be made between free respiration and artificial ventilation. When the patient is anesthetized he is placed under artificial ventilation. The ventilator is a mechanical device that controls the airflow into the patient's lungs thanks to endotracheal intubation. Since the respiration is forced by this machine, its cycle is perfectly periodic. Ventilation may be mandatory when the drugs that are used to anesthetize the patient block the respiratory muscles. If the patient is able to breathe freely, then the motion secondary to respiration is no longer strictly periodic [28].

The internal motion of the organs can be very different from external motion of the abdomen, so external measurements are not sufficient. If internal measurements cannot be obtained in real time, a correlation model must be used that gives the relationship between external and internal data, as in [28-30]. For example, the Cyberknife (Accuray, Sunnyvale, CA) is a linear accelerator mounted on a 6-dof manipulator, designed to destroy tumors using radiotherapy. Schweikard *et al.* [29] describe a solution to track the tumor in real time using the Cyberknife system. They use the combination of two kinds of sensors—a pair of X-ray cameras and an infrared tracking system—to compute a deformation model which describes the correlation between the motion of internal gold markers and external infrared markers. This model is used to obtain the positions of the internal gold markers attached to the target organ with a high refresh rate (60 Hz) even with a very slow X-ray imaging system (0.1 Hz). This measurement is then used to control the robot which compensates for the respiration-induced motion of the tumor.

In percutaneous interventions, a needle is inserted into the patient, its path guided by some medical imaging modality (e.g., ultrasound, X-rays, computed tomography or magnetic resonance). The needle tip is brought to the center of a tumor which is destroyed using thermo-ablation. Manual interventions expose the physician to high doses of radiation. Therefore, telemanipulated robotic needle holders have been recently developed [31]. These systems should, of course, be able to compensate for physiological motions in order to guarantee a constant positioning at the center of the tumor.

A simple passive means for respiratory motion

compensation in percutaneous procedures is to put the robot on the patient. For example, the CT-bot [32] is a little robotic needle driver that attaches to the patient. This way, some components of respiratory motions can be attenuated. Furthermore, the risk of injuries due to other accidental body motions of the patient is far lower than with a table-mounted robot.

In laparoscopic robotic surgery, endoscopic imaging can be used to measure intraoperative internal motions. This information can be used to track the moving organ. A stabilized image can be fed to the surgeon who can concentrate on the useful task while letting the system autonomously and transparently compensate for respiratory motions.

A. Motion Acquisition and Analysis

Typical motion resulting from respiration is presented in Fig. 5. The plot gives the measured distance between the tip of a laparoscopic instrument and the surface of the liver of an anesthetized, artificially ventilated pig. This measurement was estimated from the endoscopic image with the reconstruction method described in [1]. The acquisition frequency is 25 Hz. In this experiment, the instrument is static so the variation of the distance is only due to the motion of the liver. The plot shows clearly that the disturbance due to respiration is quasi-periodic. This property was exploited by Riviere *et al*. for prediction of respiratory motion using the WFLC algorithm [33]. For the same reason, the research team of Drs. Gangloff and Mathelin has utilized repetitive control techniques, as described in the remainder of this section.

B. Repetitive Control

Repetitive control is a well-known technique in control theory that can be used to drastically improve tracking performance in the presence of quasi-periodic disturbances. This technique is used, for example, to compensate for eccentricities in the servo loop that keeps a laser following a track on a CD or DVD. Respiratory motion is a good candidate for such a control scheme: the algorithm is able to adaptively learn the shape of the disturbance and to perfectly reject it after this learning phase.

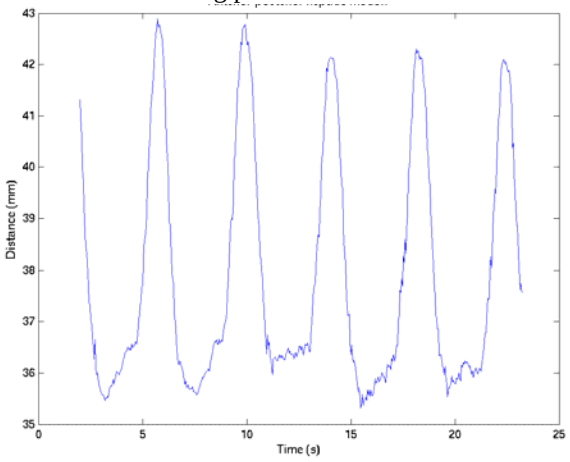

Fig. 5. Measurement of the motion of a pig's liver secondary to respiration

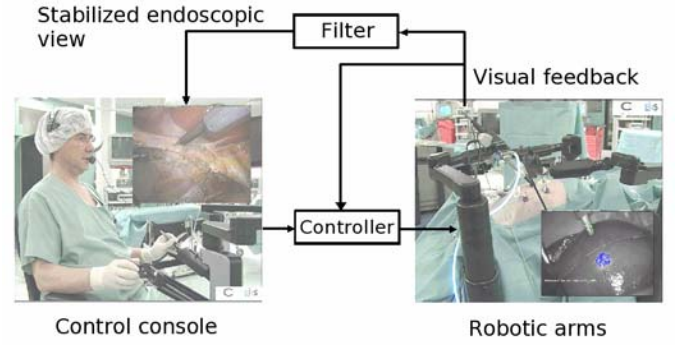

Fig. 6. System overview

Fig. 6 gives an overview of what would be an active motion compensation system in laparoscopic surgery. The goal is to give the surgeon who telemanipulates the feeling that he is operating on an organ that is perfectly still so he can concentrate only on the useful task.

The local loop, having the endoscopic video signal as feedback, uses a repetitive controller to track the organ. Reference signals coming from the surgeon's master console generate "reference-following" control signals that are added to the "disturbance-rejection" control signals.

A modified version of the Generalized Predictive Controller (GPC) [34], called R-GPC (the "R" stands for Repetitive), was developed for this application: this controller separates the reference-following component from the disturbance-rejection component in such a way that there are no more cross-coupling effects, with the same rejection performances than standard repetitive control. Furthermore, it is possible to tune separately the performance of the two components, which is not possible when using standard repetitive control.

The experimental setup that was used to validate the R-GPC approach is described in Fig. 7. An Aesop robot from Computer Motion is used to control the position of a tool. This tool is equipped with optical markers to measure the distance y between the tip of the instrument and the surface of the organ (see [1] for a more detailed explanation of the system). A visual servo-loop running at the endoscopic video frame rate (25 Hz) controls y toward a desired reference signal.

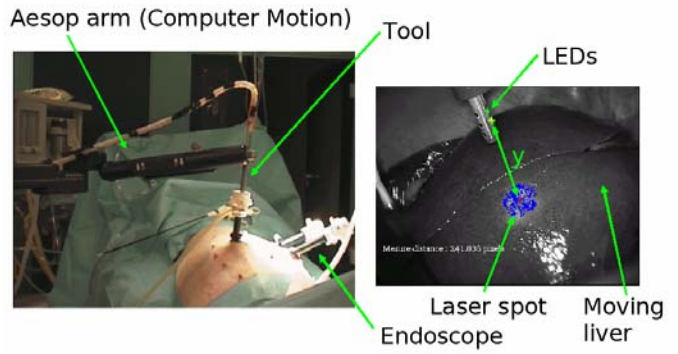

Fig. 7. Respiratory motion compensation using R-GPC

The experiment was carried out on an anesthetized pig. In Fig. 8 we compare the response of the system with a standard GPC (without the repetitive feature) and an R-GPC. The GPC

and the R-GPC are tuned to achieve the best trade-off between stability and performance. The pixel/distance ratio is about 5 pixels/mm. A step is performed on the reference to simulate the action of the surgeon. These figures clearly show the superiority of the repetitive strategy. With the R-GPC, the maximal error is reduced by a factor of 2.5 with respect to standard GPC, leaving a residual motion of about 1 mm, which is accurate enough to potentially improve a wide range of surgical gestures.

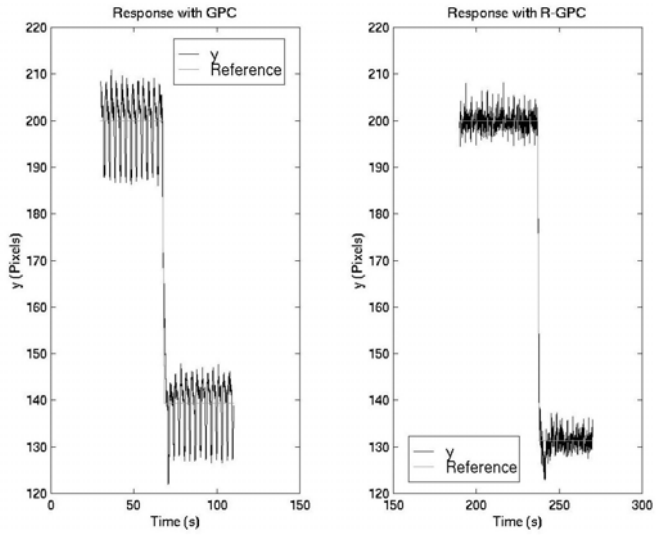

Fig. 8. *In vivo*: regulation of *y* with GPC and R-GPC

IV. HEARTBEAT

Heart surgery presents unique difficulties: various tasks, some requiring high accuracy (≈100 μm), must be performed on an organ that is beating rhythmically at a frequency of roughly 1 Hz and an amplitude of 1 cm or more. To overcome this problem, the heart often is arrested and the blood circulation maintained by an external pump. But extracorporeal circulation has some major drawbacks, the first being a significant risk of neurological complications [11].

On the other hand, beating heart surgery allows for operating on a heart that keeps pumping the blood. It is possible to use a mechanical stabilizer to constrain the motion of a small area on the heart surface. In open surgery, many stabilizers are available. Today, they are widely used for conventional coronary artery bypass grafting surgery (e.g., the Octopus from Medtronics in Fig. 12).

Conventional beating heart surgery remains very invasive since it requires a large opening of approximately 20 cm in the chest: the sternotomy. This yields other potential complications—mainly infection and nerve damage – due to the large wound and the retraction of the ribs. Morbidity can be drastically reduced by minimally invasive approaches in which the heart is accessed through small incisions, typically between the ribs. In this context, stopping the heart via cardiopulmonary bypass is still possible, although more difficult [35], but it still increases morbidity just as in open surgery; hence the attractiveness of beating-heart surgery.

To facilitate this, minimally invasive versions of mechanical stabilizers have been developed, which are inserted through small intercostal incisions and attached to the operating table rail. According to one study, the residual motion is significantly greater than with the open-chest versions, due to the greater flexibility of the narrow endoscopic tools and the greater distance between mounting point and worksite [36].

A. HeartLander

A more sophisticated option for passive compensation of the heartbeat motion is a flexibly tethered robotic device that mounts to the beating heart, not constraining its motion, but moving with it as it beats freely. This has been the approach taken by the HeartLander project in Dr. Riviere's laboratory [37]. HeartLander is a miniature mobile robot, shown in Fig. 9, designed to be introduced into the pericardial sac through a minimally invasive port, adhere to the epicardial surface using suction, travel to any desired location on the epicardium, and perform treatment under the control of the surgeon.

The front body or foot of the device is attached to three superelastic nitinol wires that pass freely through the rear body and connect to the drive pulleys of three motors in a box located outside the patient. (Nitinol is used here solely for its elastic properties, not because of the well-known shape memory effect.) The three wires are spaced in a radially symmetric pattern. Each wire passes through a flexible plastic sheath, one end of which is attached to the rear body of HeartLander, and the other to a stationary block located near the motors. Provided slack is maintained in the tether, locomotion and steering can be performed by pushing and pulling the wires in a cyclic inchworm-like process as described in [38]. With each step, the seal at the suction pad of the newly placed foot is monitored using a pressure sensor located in the tabletop box in order to ensure that the foot has a good grip on the surface before initiating movement of the other foot.

Visual feedback is provided by a 3.8-mm diameter fiber

Fig. 9. HeartLander. Suction is applied to each of the two round feet in order to adhere to the epicardium. The device crawls like an inchworm, using wires to advance the front foot and then sheaths surrounding the wires to push the rear foot up to meet the front. Steering is performed by advancing unequal lengths of the three wires. The device includes a videoscope for visual feedback, and is controlled via joystick by the surgeon. Numerous end-effectors are possible; the prototype shown incorporates a retractable needle for injections (shown partially extended for visibility).

optic endoscope running through the tether, which provides an image resolution of 510 x 492 pixels. The control program makes the locomotion kinematics transparent to the surgeon, who simply commands the device to travel forward, backward, left, or right using a joystick. The speed of travel depends upon step length, step velocity, and step efficiency (or amount of slip per step). The maximum speed recorded while traveling across the anterior surface of a synthetic beating heart model was 0.003 m/s over a distance of 10 cm. The system is capable of submillimeter precision in locomotion. The needle in the present prototype is manually controlled, although computerized control would be possible using the same joystick used for locomotion.

HeartLander has been tested *in vivo* in three porcine trials [38]. Median sternotomy was performed on these pigs, but the pericardial sac was left intact. HeartLander was introduced into the thoracic cavity through a 15-mm port, placed so as to simulate subxiphoid access, and applied to the epicardial surface through a 10-mm incision in the pericardium. The device was able to maintain prehension of the beating myocardium despite the overhead contact with the pericardium. Locomotion was achieved across several surfaces including the anterior wall of the beating right ventricle, the anterolateral wall of the beating left ventricle, and the anterior wall of the left atrial appendage (Fig. 10). The pericardium is translucent, and locomotion trials were recorded using a handheld video camera.

Myocardial injections of tissue-marking dye (0.5 cc) were performed at two locations [38]. In each case, HeartLander walked to the planned site, and a stable platform for operation was then established by applying suction to both feet. The surgeon then advanced the needle into the myocardium and performed the injection. No bleeding was observed following needle withdrawal. Confirmation of successful injection was made during postoperative examination of the excised porcine hearts. Following all procedures, the surgeon confirmed that no damage was done to the myocardium or pericardium.

HeartLander compensates the disturbance due to the heartbeat by adhering to the heart, locating itself in the moving frame of reference of the heart surface. Because of its flexible tether and its locomotion capability, the pericardial incision no longer need be located near the epicardial site where therapy is to be applied. As a result, instead of the transthoracic approach typically used for rigid endoscopic cardiac instruments, HeartLander can be introduced through an incision below the xiphoid process of the sternum. This not only obviates sternotomy and cardiopulmonary bypass, but avoids entering the pleural space altogether. As a result, unlike transthoracic access, deflation of the left lung is not needed and it becomes feasible to use local or regional rather than general anesthetic techniques. This has the potential to open the way to ambulatory outpatient cardiac surgery for procedures such as atrial ablation, epicardial electrode placement, and myocardial injection of drugs or cells for tissue regeneration.

B. Active Heart Motion Compensation

Since 2000, several research teams, including that of Drs. Gangloff and Mathelin in Strasbourg, have begun to study the difficult problem of active heart motion compensation. Nakamura *et al.* [39] developed a mini-robot attached to the sternal retractor that is able to track a marker on a beating heart using high-speed visual servoing. They introduced the concept of "heartbeat synchronization." The idea is to give the surgeon the feeling that he is operating on a virtually stabilized organ, letting the robot compensate for the beating motion and providing a stabilized visual feedback of the scene. In this experiment, the control law does not take into account the repetitive nature of the disturbance. Ortmaier [40] worked on robust real-time feature extraction. He proposed an algorithm to track the motion of the heart in an image using the repetitive properties. Robotic applications were presented as future work.

Typical heart motions are presented in Fig. 11. These measurements were taken on a pig's heart which is an accepted model of the human's heart. Note the two distinct components: a slow one at ≈0.25 Hz due to respiration and a faster one with sharp transients which reflects the beating at ≈1 Hz. A better knowledge of the heart motion (e.g., acceleration, amplitude, waveform) would greatly improve the design of an active filtering system for 3 main reasons:

1. It can be taken into account in a predictive control scheme.
2. It would help to define more accurately the specifications of the dedicated mechanical structure.
3. It would increase safety by allowing input signals to be checked for the expected characteristics.

Cattin *et al.* [41] assess the significance of the residual motion after stabilization of a pig's beating heart with an Octopus. The repeatability of the stabilized cardiac motions, providing that hemodynamics are constant, is underlined but no model is proposed. In [42], Fourier coefficients of both components are estimated by a two-stage adaptive algorithm. A similar approach based on adaptive filtering to separate the two components and predict future motion is presented in [43]. These approaches are frequency-based and they assume that the model of the heart is invariant.

Additional measurement signals can be used to predict more efficiently the cardiac motion. In [40], ECG signals and ventilator air pressure are used to improve the tracking of landmarks in the image of a beating heart. In [44], the Strasbourg team uses ECG signals, ventilator airflow and high-speed imaging to precisely assess the heart motion and improve drastically the prediction of the heart's motion. The remainder of this section details the results obtained in this work.

The setup used to assess the motion of the heart is shown in Fig. 12. Optical markers (four LEDs) are affixed to the myocardium of an anesthetized pig that underwent a sternotomy. A 500 Hz high-speed camera with a 256×256-pixel grayscale sensor (DALSA CAD6) is placed on a tripod,

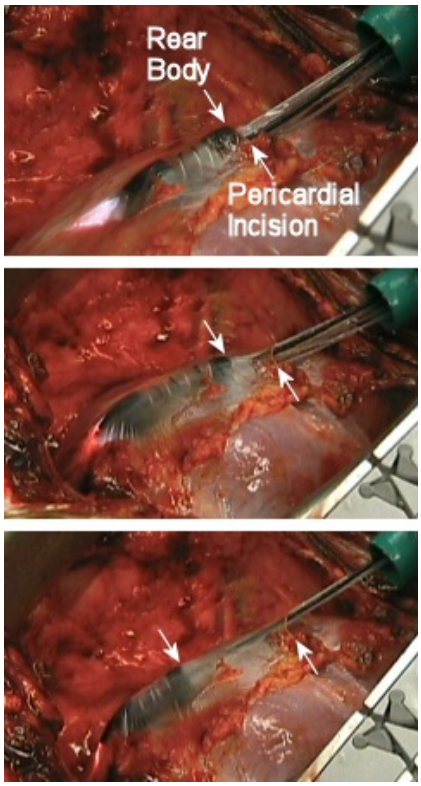

Fig. 10. Time sequence showing HeartLander walking across a beating porcine heart inside the pericardial sac. The lower arrow indicates the location of the pericardial incision; the upper arrow indicates the rear foot of the device.

its lens focused on the optical markers. The 3D position of the heart can be computed accurately from the marker positions in the image using standard pose reconstruction techniques. ECG signals are acquired through a classical 3-lead ECG cable and a custom-made differential amplifier with a gain of 1000. This simple amplifier that uses the AD624 instrumental amplifier (Analog Devices) was built in order to avoid the 20- to 25-ms delay of commercial ECGs due to built-in signal post-processing. Two AWM700 airflow sensors from Honeywell were used for the real-time measurement of the ventilator flow. Both ECG signals and airflow measurements are acquired at 500 Hz by a PCI acquisition board synchronized with the image acquisition. The complete acquisition software runs on RTAI [http://www.rtai.org], an open-source real-time operating system, in order to ensure perfect synchronization and minimal jitter.

The heart trajectory is complex but repetitive. In Fig. 13, respiration is stopped: each beating cycle follows almost exactly the same 3D path. Furthermore, this same figure gives some clues about the residual motion after stabilization. By differentiating the position readings we were able to estimate quite precisely the velocity and acceleration of the myocardium. In normal conditions (no stabilization, 60 bpm), the peak velocity was observed in the sagittal plane: more than 0.1 m/s. The highest acceleration was also in this plane: up to 10 m/s^2. After an injection of adrenaline, the beating frequency increased to 200 bpm. In this state, we measured a peak velocity of 0.2 m/s and maximum acceleration of 20 m/s^2.

It should also be pointed out that there is a coupling between beating motion and respiration: the heart motion waveform varies depending on where the heartbeat occurs in the respiration cycle. It is mainly the amplitude of the beating that is altered by the volume of the lungs. Linear Parameter Variant (LPV) techniques can be used to model this effect as shown in Fig. 11, in which the prediction accuracy of an LPV method is compared to a frequency method (as in [43]).

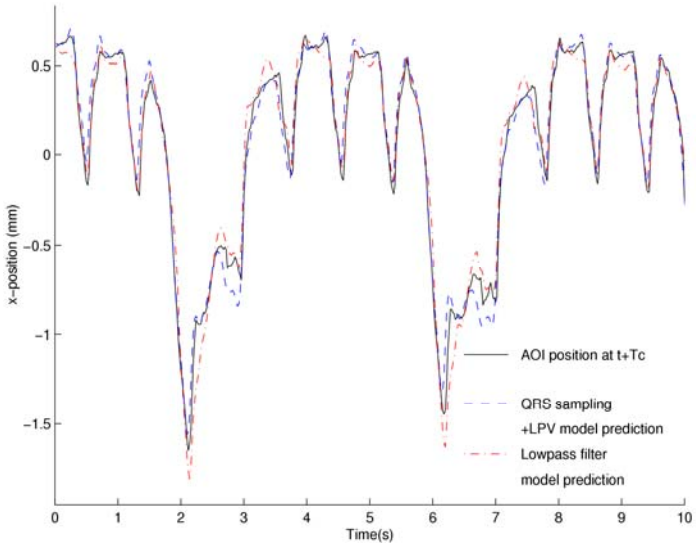

Fig. 11. Typical heart motion and prediction results.

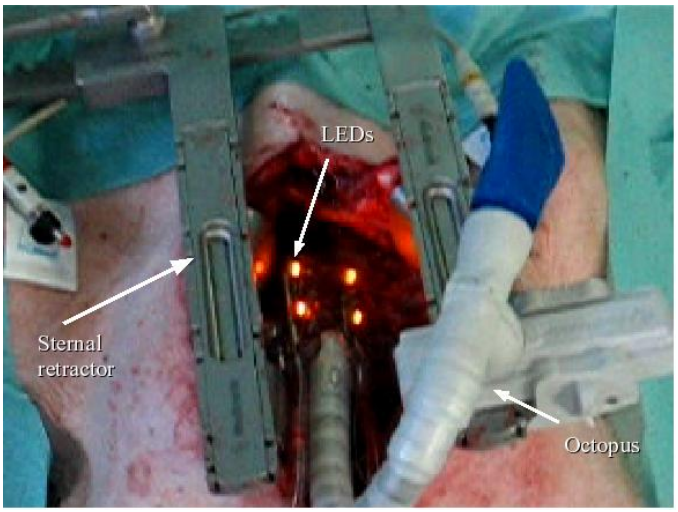

Fig. 12. The heart stabilizer OCTOPUS and its visual markers

The injection of anesthetizing drugs has a stabilizing effect on the heart, but arrhythmias can occur. In a compensation system based on prediction, arrhythmic motions are disturbances that must be detected before they happen in order to put the system in a failsafe mode. The Strasbourg team showed in [44] that abnormal ECG signals always precede abnormal motions, by 80 ms on average. This is quite enough to let the robot move to a safe position that would prevent any damage to the heart.

Experimental validations of the predictive approach to heart

motion compensation were carried out at IRCAD in Strasbourg on a laboratory testbed and finally on a pig's heart. The laboratory setup is shown in Fig. 14.

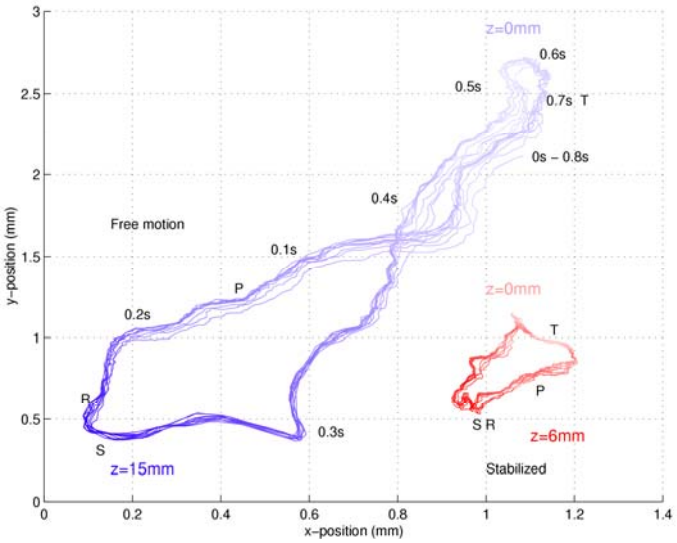

Fig. 13. Heart trajectories in 3D space with no ventilation (time parameterization, depth z coded in color intensity)

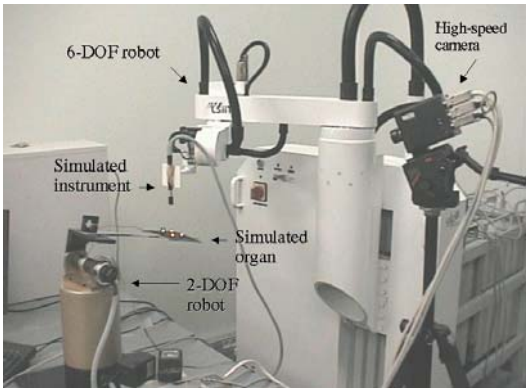

Fig. 14. Active heart motion compensation (testbed).

In this system, high-speed visual servoing (500 Hz sampling rate) is used to enable robotic tracking of optical markers on the surface of a simulated heart. The high sampling rate is necessary to avoid aliasing in the measurement of the heart motion (high frequency components due to sharp transients) and to ensure a high bandwidth for the visual servo loop.

For the experiment *in vivo*, the optical markers were attached to the myocardium of the pig as shown in Fig. 15.

Model Predictive Control (MPC) [45] is used with a motion predictor to predict the behavior of the heart: control signals are sent to the robot in advance to compensate for future (expected) changes in the measurements (image features). The plot in Fig. 16 shows the tracking error function of time. Predictive control is switched on at t=17s, yielding a clear improvement in the tracking error. The pixel/distance ratio is about 40 pixels/cm, so the residual relative motion amplitude is about 1.5 mm peak-to-peak. The accuracy needed for coronary artery surgery is about 0.2 mm. To reach this goal, the Strasbourg team is currently working on improving the accuracy of a predictive model of the heart which has already given some promising results [44].

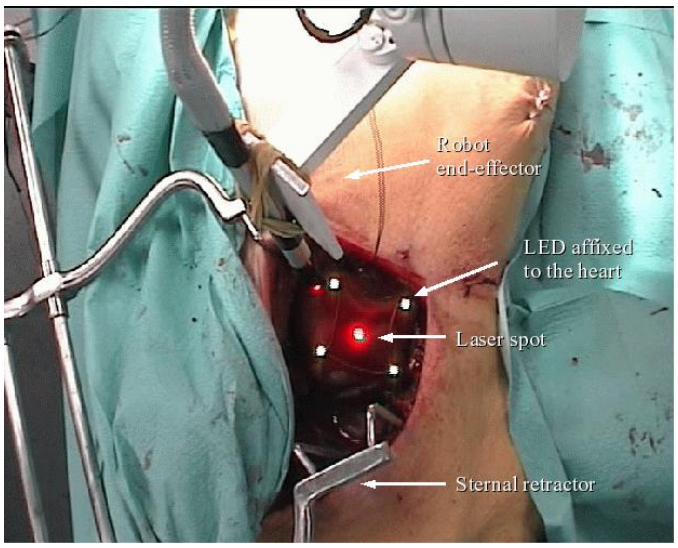

Fig. 15. Active heart motion compensation (*in vivo*).

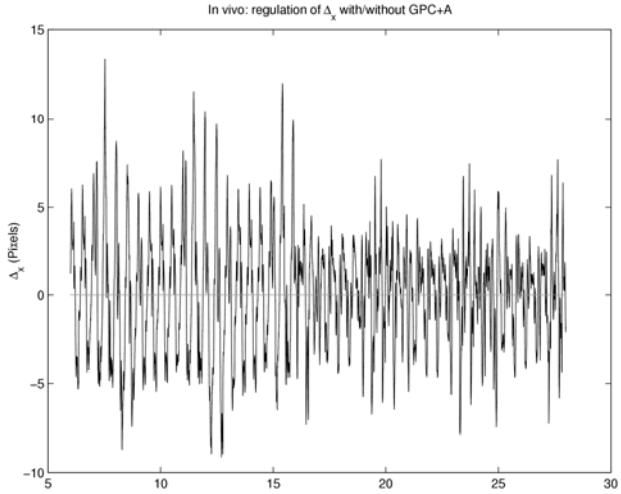

Fig. 16. Tracking error (*in vivo*).

V. Discussion

All these applications follow a recent trend in surgical robotics: future surgical robotic systems will no longer be adaptations of industrial robots to the medical field or systems that duplicate the surgeon's gestures, but increasingly systems will be dedicated to a single task, usually miniaturized, with some autonomous capabilities and an extreme level of safety. Most likely they will conform less and less to what is usually thought of as a robot; instead they will be considered more like smart surgical instruments, advanced tools providing the surgeon with new capabilities for minimally invasive surgery.

These projects have demonstrated the feasibility of robotic compensation of biological motion, but the research has not yet made its way to the clinic. In the case of active compensation systems, their autonomous operation represents a safety issue over and above those already faced by telerobotic systems.

Continued research is needed in each of the projects presented here. In microsurgery, the level of accuracy required places heavy demands on the system. Further refinements in sensor signal processing are underway for Micron, as well as integration with video tracking systems in the stereo microscope that can provide redundant sensing. Future work with HeartLander involves continued efforts at miniaturization and development of new types of end-effectors in preparation for fully closed-chest porcine tests *in vivo*. Repetitive control for respiratory motion compensation will be integrated with the patient-mounted "CT-bot" robot and ultra-sound guidance in order to compensate for internal organ motions in percutaneous surgery. Future work in robotized beating heart surgery will mainly focus on the mechanical design of a dedicated minimally-invasive robotized instrument that will have several internal actuated degrees of freedom and additional sensory capabilities such as force feedback. The smaller this mechanical structure will be and the safer it will be for the patient and also for the surgical staff.

More generally, however, in order to take these proofs of concept and move them to the clinic, further development is needed in order to produce systems that are robust, safe, compatible with other equipment, and easy for medical personnel to use. These goals can best be accomplished by commercial partners interested in the work.

ACKNOWLEDGMENT

C. Riviere thanks S. Y. Khoo, W. T. Ang, N. Patronik, D. Choi, and Drs. M. Zenati and S. El-Qarra. J. Gangloff and M. de Mathelin thank Professor J. Marescaux, L. Soler, M. A. Sanchez and A. Forgione from IRCAD in Strasbourg for their support in the experimental part of their work, as well as their past and current Ph.D. students involved in this research: R. Ginhoux and L. Cuvillon.

REFERENCES

[1] A. Krupa, J. Gangloff, C. Doignon, M. F. de Mathelin, G. Morel, J. Leroy, L. Soler, and J. Marescaux, "Autonomous 3-D positioning of surgical instruments in robotized laparoscopic surgery using visual servoing," *IEEE Trans. Rob. Autom*., vol. 19, pp. 842-853, Oct. 2003.

[2] Y. Wang, S. J. Riederer, R. L. Ehman, "Respiratory motion of the heart: kinematics and the implications for the spatial resolution in coronary imaging," *Magn. Reson. Med*., vol. 33, pp. 713-719, May 1995.

[3] M. A. Clifford, F. Banovac, E. Levy, and K. Cleary, "Assessment of hepatic motion secondary to respiration for computer assisted interventions," *Comput. Aided Surg*., vol. 7, no. 5, pp. 291–299, 2002.

[4] S. B. Solomon, A. Patriciu, M. E. Bohlman, L. R. Kavoussi, D. Stoianovici, "Robotically driven interventions: a method of using CT fluoroscopy without radiation exposure to the physician," *Radiology*, vol. 225, pp. 277-282, Oct. 2002.

[5] M. Engelsman, E. M. Damen, K. De Jaeger, K. M. van Ingen, and B. J. Mijnheer, "The effect of breathing and set-up errors on the cumulative dose to a lung tumor," *Radiother. Oncol*., vol. 60, no. 1, pp. 95-105, 2001.

[6] J. M. Balter, R. K. Ten Haken, T. S. Lawrence, K. L. Lam, and J. M. Robertson, "Uncertainties in CT-based radiation therapy treatment planning associated with patient breathing," *Int. J. Radiat. Oncol. Biol. Phys*., vol. 36, no. 1, pp. 167-174, 1996.

[7] D. S. Siganos, K. A. Evangelatou, T. G. Papadaki, V. J. Katsanevaki, A. I. Dagos, and I. G. Pallikaris, "Photorefractive keratectomy in eyes with congenital nystagmus," *J. Refract. Surg.*, vol. 14, pp. 649-652, Nov./Dec. 1998.

[8] M. Mrochen, M. S. Eldine, M. Kaemmerer, T. Seiler, and W. Hutz, "Improvement in photorefractive corneal laser surgery results using an active eye-tracking system," *J. Cataract Refract. Surg.*, vol. 27, pp. 1000-1006, Jul. 2001.

[9] R. C. Harwell and R. L. Ferguson, "Physiologic tremor and microsurgery," *Microsurgery*, vol. 4, pp. 187-192, 1983.

[10] M. Patkin, "Ergonomics applied to the practice of microsurgery," *Aust. N. Z. J. Surg*., vol. 47, pp. 320–239, 1977.

[11] G. W. Roach, M. Kanchuger and C. M. Mangano. Adverse cerebral outcomes after coronary bypass surgery. *N. Engl. J. Med.,* vol. 335, pp. 1857-1863, 1996.

[12] D. Y. Loisance, K. Nakashima and M. Kirsch. Computed-assisted coronary surgery: lessons from an initial experience. *Interactive Cardio Vasc. Thorac. Surg.,* vol. 4, pp. 398-401, 2005.

[13] R. J. Elble and W. C. Koller, *Tremor*. Baltimore: Johns Hopkins University Press, 1990.

[14] F. Peral-Gutierrez, A. L. Liao, and C. N. Riviere, "Static and dynamic accuracy of vitreoretinal surgeons," in *Proc. 26th Annu. Int. Conf. IEEE Eng. Med. Biol. Soc*., 2004, pp. 2734-2737.

[15] C. Gantert, J. Honerkamp, and J. Timmer, "Analyzing the dynamics of hand tremor time series," *Biol. Cybern*., vol. 66, pp. 479-484, 1992.

[16] M. J. Elman, J. Sugar, R. Fiscella, T. A. Deutsch, J. Noth, M. Nyberg, K. Packo, R. J. Anderson, "The effect of propranolol versus placebo on resident surgical performance," *Trans. Am. Ophthalmol. Soc.*, vol. 96, pp. 283-291, 1998.

[17] H. Das, H. Zak, J. Johnson, J. Crouch, and D. Frambach, "Evaluation of a telerobotic system to assist surgeons in microsurgery," *Comput. Aided Surg*., vol. 4, pp. 15-25, 1999.

[18] P. S. Jensen, K. W. Grace, R. Attariwala, J. E. Colgate, M. R. Glucksberg, "Toward robot-assisted vascular microsurgery in the retina," *Graefes Arch. Clin. Exp. Ophthalmol.*, vol. 235, pp. 696-701, Nov. 1997.

[19] I. W. Hunter, T. D. Doukoglou, S. R. Lafontaine, P. G. Charette, L. A. Jones, M. A. Sagar, G. D. Mallinson, and P. J. Hunter, "A teleoperated microsurgical robot and associated virtual environment for eye surgery," *Presence*, vol. 2, pp. 265-280, 1993.

[20] R. Taylor, P. Jensen, L. Whitcomb, A. Barnes, R. Kumar, D. Stoianovici, P. Gupta, Z. Wang, E. de Juan, Jr., and L. Kavoussi, "A steady-hand robotic system for microsurgical augmentation," *Int. J. Robot. Res*., vol. 18, pp. 1201-1210, 1999.

[21] C. N. Riviere, W. T. Ang, and P. K. Khosla, "Toward active tremor canceling in handheld microsurgical instruments," *IEEE Trans. Rob. Autom*., vol. 19, pp. 793-800, Oct. 2003.

[22] W. T. Ang, P. K. Khosla, and C. N. Riviere, "Design of all-accelerometer inertial measurement unit for tremor sensing in handheld microsurgical instrument," in *Proc. IEEE Int. Conf. Rob. Autom*., Taipei, Taiwan, 2003, pp. 1781-1786.

[23] C. N. Riviere and N. V. Thakor, "Adaptive human-machine interface for persons with tremor," in *Proc. 17th Annu. Conf. IEEE Eng. Med. Biol. Soc*., Montréal, 1995, pp. 1193-1194.

[24] M. Bodson and S. C. Douglas, "Adaptive algorithms for the rejection of periodic disturbances with unknown frequency," in *Proc. 13th World Congr. Int. Fed. Autom. Contr*., San Francisco, 1996, vol. K, pp. 229-234.

[25] M. Bodson and S. C. Douglas, "Adaptive algorithms for the rejection of sinusoidal disturbances with unknown frequency," *Automatica*, vol. 33, no. 12, pp. 2213–2221, 1997.

[26] C. N. Riviere, R. S. Rader, and N. V. Thakor, "Adaptive canceling of physiological tremor for improved precision in microsurgery," *IEEE Trans. Biomed. Eng*., vol. 45, pp. 839-846, July 1998.

[27] D. Y. Choi and C. N. Riviere, "Flexure-based manipulator for active handheld microsurgical instrument," in *Proc. 27th Annu. Int. Conf. IEEE Eng. Med. Biol. Soc*., Shanghai, to be published.

[28] S. Dieterich, J. Tang, J. Rodgers, and K. Cleary, "Skin respiratory motion tracking for stereotactic radiosurgery using the cyberknife," in *Proc. Int. Conf. Comput. Assist. Radiol. Surg.*, London, 2003, pp. 130–136.

[29] A. Schweikard, G. Glosser, M. Bodduluri, M. Murphy, and J. Adler, "Robotic motion compensation for respiratory motion during radiosurgery," *Comput. Aided Surg.*, vol. 5, no. 4, pp. 263–277, Sept. 2000.

[30] J. Tang, S. Dieterich, and K. Cleary, "Respiratory motion tracking of skin and liver in swine for cyberknife motion compensation," in *SPIE Medical Imaging*, vol. 5367, 2004, pp. 729–734.

[31] D. Stoianovici, K. Cleary, A. Patriciu, D. Mazilu, A. Stanimir, N. Craciunoiu, V. Watson, L. Kavoussi, "AcuBot: a robot for radiological interventions," in *Proc. IEEE Int. Conf. Rob. Autom*., Taipei, Taiwan, 2003, pp. 927-930.

[32] B. Maurin, C. Doignon, J. Gangloff, B. Bayle, M. de Mathelin, O. Piccin, and A. Gangi, "Ct-bot: A stereotactic-guided robotic assistant for percutaneous procedures of the abdomen," in *SPIE Medical Imaging*, San Diego, Feb. 2005.

[33] C. N. Riviere, A. Thakral, I. I. Iordachita, G. Mitroi, and D. Stoianovici, "Predicting respiratory motion for active canceling during percutaneous needle insertion," in *Proc. 22nd Annu. Conf. IEEE Eng. Med. Biol. Soc*., Istanbul, 2001, pp. 3477-3480.

[34] D. W. Clarke, C. Mohtadi, and P. S. Tuffs, "Generalized predictive control - part 1. The basic algorithm," *Automatica*, vol. 23, pp. 137–160, 1987.

[35] H. Vanermen, F. Wellens, R. De Geest, I. Degrieck, and F. Van Praet, "Video-assisted port-access mitral valve surgery: from debut to routine surgery. will trocar-port-access cardiac surgery ultimately lead to robotic cardiac surgery? " *Sem. Thorac. Cardiovasc. Surg.*, vol. 11, no. 3, pp. 223–234, July 1999.

[36] P. F. Gründeman, R. Budde, H. M. Beck, W.-J. van Boven, and C. Borst, "Endoscopic exposure and stabilization of posterior and inferior branches using the endo-starfish cardiac positioner and the endo-octopus stabilizer for closed-chest beating heart multivessel cabg: Hemodynamic changes in the pig," *Circulation*, vol. 108, no. 10, pp. II34–II38, Sept. 2003.

[37] C. N. Riviere, N. A. Patronik, and M. A. Zenati, "A prototype epicardial crawling device for intrapericardial intervention on the beating heart," *Heart Surg. Forum*, vol. 7, no. 6, pp. E639-E643, 2004.

[38] N. Patronik, M. A. Zenati, and C. Riviere, "Preliminary evaluation of a mobile robotic device for navigation and intervention on the beating heart," *Comput. Aided Surg.*, vol. 10, no. 4, 2005, in press.

[39] Y. Nakamura, K. Kishi, and H. Kawakami, "Heartbeat synchronization for robotic cardiac surgery," in *Proc. IEEE Int. Conf. Rob. Autom.*, Seoul, Korea, 2001, vol. 2, pp. 2014-2019.

[40] T. J. Ortmaier, "Motion compensation in minimally invasive robotic surgery," Ph.D. dissertation, T. U. München, 2003. [Online]. Available: http://tumb1.biblio.tu-muenchen.de/publ/diss/ei/2003/ortmaier.html

[41] P. Cattin, H. Dave, J. Grünenfelder, G. Szekely, M. Turina, and G. Zünd, "Trajectory of coronary motion and its significance in robotic motion cancellation," *European Journal of Cardio-Thoracic Surgery*, vol. 25, pp. 786–790, 2004.

[42] A. Thakral, J. Wallace, D. Tomlin, N. Seth, and N. V. Thakor, "Surgical motion adaptive robotic technology (S.M.A.R.T.): Taking the motion out of physiological motion," in *Proc. 4th Int. Conf. Med. Image Comput. Comput. Assist. Intervention (MICCAI)*, Utrecht, Netherlands, 2001, pp. 317–325.

[43] R. Ginhoux, J. Gangloff, M. de Mathelin, L. Soler, M. A. Sanchez, and J. Marescaux, "Active filtering of physiological motion in robotized surgery using predictive control," *IEEE Trans. Rob.*, vol. 21, no. 1, pp. 67–79, Feb. 2005.

[44] L. Cuvillon, J. Gangloff, A. Forgione, E. Laroche, and M. de Mathelin, "Toward robotized beating heart TECABG: assessment of the heart dynamics using high-speed vision," in *Proc. Int. Conf. Med. Image Comput. Computer-Assisted Intervention*, Palm Springs, California, USA, Oct. 2005.

[45] E. F. Camacho and C. Bordons, *Model Predictive Control*. London: Springer-Verlag, 1999.